ENGINEER - Vol. LIX, No. 02, pp. [01-10], 2026

DOI: https://doi.org/10.4038/engineer.v59i2.7744

Development of a Point Absorber Type Wave Energy Converter Optimised for Sri Lankan Wave Conditions

K.G.S.M. Rathnapriya, R.G.P.D. Rankothge, R.R. Gamage, W.A.D. Sampath, I.H.D. Seneviratne and H.C.P. Karunasena

Abstract: Wave energy is recognized as a renewable energy resource with a comparatively high energy density relative to other renewable sources; however, its large-scale exploitation remains limited due to technological, economic, and deployment challenges. As a result, only a small number of wave energy converters (WECs) have been successfully implemented worldwide. This study presents the development and field testing of a double-buoy, point absorber type WEC incorporating a dual rack-and-pinion power take-off (PTO) mechanism, designed for deployment in nearshore sea conditions. The hydrodynamic performance of the proposed WEC was analysed using ANSYS AQWA to evaluate heave response, phase variation and hydrostatic forces for different floater geometries, while the structural integrity of the system was assessed using finite element analysis (FEA). Field experiments were conducted at the old harbour premises in Galle, Sri Lanka (6.029230° N, 80.219010° E), where the average significant wave height was approximately 0.3 m, with dominant wave frequencies in the range of 0.1–0.3 Hz. Numerical predictions were compared with gathered experimental measures to validate the model. Experimental results indicated a peak power output of approximately 60 W and an average power output of around 15 W with an estimated overall conversion efficiency of 8.51% under the tested wave conditions. Future work will focus on improving the power-to-weight ratio and eliminating the bottom counterweight, enabling deployment in variable water depths and enhancing the adaptability of the WEC for broader coastal applications.

Keywords: Double Buoy, Point Absorber, Renewable Energy, Sustainable, Wave Energy Converter

1. Introduction

Energy underpins modern civilization, yet global demand is still dominated by fossil fuels, leading to environmental degradation and climate change. This has intensified the need for sustainable renewable energy sources. Among them, wave energy is particularly promising due to its high energy density and predictability. The Intergovernmental Panel on Climate Change (IPCC) estimates that global wave energy resources have the theoretical potential to generate approximately 29,500 TWh annually, indicating its capacity to become a major future energy source [1]. Also, Marine Power Systems projects that wave energy could supply up to 10% of global electricity demand by 2050 [2].

Wave energy converters (WECs) are used to convert kinetic and potential energy of ocean waves into electricity. According to the European Marine Energy Centre (EMEC), WECs are classified into several categories, including attenuators, point absorbers, oscillating wave surge converters, oscillating water columns, and overtopping devices [3]. Among these, point absorbers are the most commonly studied due to their compact

Mr. K.G.S.M. Rathnapriya, Department of Mechanical and Manufacturing Engineering, Faculty of Engineering, University of Ruhuna, Hapugala, Galle, Sri Lanka
Email: sadeeramandara81@gmail.com
https://orcid.org/0009-0005-5425-8984
Mr. R.G.P.D. Rankothge, Department of Mechanical and Manufacturing Engineering, Faculty of Engineering, University of Ruhuna, Hapugala, Galle, Sri Lanka
Email: praveendhanwantha@gmail.com
Mr. R.R. Gamage, Department of Mechanical and Manufacturing Engineering, Faculty of Engineering, University of Ruhuna, Hapugala, Galle, Sri Lanka
Email: ravijayagamage@gmail.com
Mr. W.A.D. Sampath, Department of Mechanical and Manufacturing Engineering, Faculty of Engineering, University of Ruhuna, Hapugala, Galle, Sri Lanka
Email: sampathwad98@gmail.com
Eng. I.H.D. Seneviratne, AMIE(SL), Department of Mechanical and Manufacturing Engineering, Faculty of Engineering, University of Ruhuna, Hapugala, Galle, Sri Lanka
Email: ihirunseneviratne@icloud.com
https://orcid.org/0009-0000-4573-089X
Eng. (Prof.) H.C.P. Karunasena, AMIE(SL), AEng, PhD (QUT), MSc (Moratuwa), BSc. Eng. (Hons.) (Moratuwa), Professor, Department of Mechanical and Manufacturing Engineering, Faculty of Engineering, University of Ruhuna, Hapugala, Galle, Sri Lanka.
Email: chaminda@mme.ruh.ac.lk
https://orcid.org/0000-0002-4203-831X

structure, omnidirectional wave response, and adaptability to varying sea states. Wave energy exhibits higher predictability than wind energy [4] and offers additional economic, social, and environmental benefits, including job creation, low environmental impact, and reduced carbon emissions. As an island nation, Sri Lanka has considerable wave energy potential, with an average annual wave power density of approximately 12–15 kW/m, particularly along its southern and western coasts [5]. Despite this, no commercially operational WECs exist in the country. Globally, WECs are challenged by issues of reliability, survivability, and cost-effectiveness [6]. However, the Department of Mechanical and Manufacturing Engineering (DMME), University of Ruhuna (UOR), has previously tested several WECs under different working principles such as "SamudraGEN" [7], a single buoy point absorber and also on-shore WECs resulting efficiencies around 4.143% [8]. Previous WEC experiments performed on point absorbers have often lacked fully sealed underwater sections, leading to potential water ingress and reliability issues as well.

To address these gaps, the present study aims to develop and validate a double-buoy, point absorber WEC on the southern coast of Sri Lanka, through an integrated analytical, numerical and experimental approach, providing essential performance data to support future large-scale wave energy deployment. Specific objectives of the study are to design a WEC, evaluate the hydrodynamic performance of the floater using numerical simulations in ANSYS AQWA, assess structural integrity through FEA, validate numerical predictions through real-world testing a fabricated model, and to determine the power output along with conversion efficiency under Southern Sri Lankan wave conditions.

2. Methodology

The wave energy converter investigated in this study, termed the Ceylon SURGE WEC, was developed using a systematic design methodology. The process began with a comprehensive review of existing WEC technologies, focusing on common failures observed during field testing. Based on this review, the WEC was developed following a systematic engineering design methodology, considering factors such as power capture motion, power take-off (PTO) mechanism, floater geometry, wave direction handling, deployment constraints, fully sealed underwater design and other aspects. A weighted evaluation process led to the selection of a double-buoy, point absorber configuration. Analytical calculations and numerical simulations were conducted to determine critical dimensions, materials, and design parameters. The dual rack-and-pinion PTO system was validated in accordance with ISO 6336:2019 standards. Finite element method (FEM) analysis was performed on major structural components using a factor of safety of 3 to ensure structural integrity for the prototype. In addition, computational fluid dynamics (CFD) simulations were carried out to optimize floater geometry, evaluating cylindrical, hemispherical, and elliptical shapes. Following design validation, fabrication proceeded from the internal PTO mechanism to the external structural components. Welding methods, structural supports, material selection, and protective coatings were verified to ensure suitability for marine environments, and the electrical system was integrated.

Laboratory testing was then conducted to verify floater motion, electrical performance, and system integration. An IoT-based monitoring system, developed using JavaScript with cloud storage via Firebase, enabled real-time measurement of voltage, current, and power output. After successful laboratory validation, sea trials were conducted to evaluate real-world performance. Experimental data were compared against predefined specifications, with design modifications implemented as necessary. Agreement between measured performance and design targets confirmed the operational feasibility of the WEC. The analytical calculations, simulations, structural validations and field-testing results formed an integrated evaluation framework ensuring the consistency between predicted and measured performance of the WEC.

3. Calculations

The WEC was analytically evaluated under similar wave conditions present in the Southern coast of Sri Lanka. An average wave height (H, crest-to-trough height) of 0.3 m and a wave period of 10 s (wave frequency of 0.1 Hz) were selected for calculation purposes. The seawater density (ρ) was taken as 1025 kg/m^3. Denoting the gravitational acceleration as 'g', the average wave energy per unit surface area (E) for a monochromatic wave train [9] is expressed as,

$$E = \frac{1}{8}\rho.g.H^2 \qquad \ldots(1)$$

This relationship provides an estimate of the theoretical energy per unit area in incoming waves. The floater's interaction with incoming waves occurs primarily through the buoyancy force variation caused by the oscillatory water surface. The time-varying vertical force acting on the floater was approximated based on linear wave theory as a hydrostatic excitation force [10] arising from variations in buoyancy as follows. Here, the waterplane area of the floating body is denoted by 'A_f', and the wave elevation at time 't' is denoted by '$\eta(t)$'.

$$F_{wave}(t) = \rho . g . A_f . \eta(t) \qquad \ldots(2)$$

For design purposes, the root mean square (RMS) force over an active half-cycle was considered which resulted in an effective wave-induced force of approximately 332 N. The floater outer diameter was taken as 880 mm and inner diameter as 700 mm. A dual rack-and-pinion mechanism was selected as the PTO system. A module 01 rack and pinion were selected where the pinion consists of 30 teeth. The rack-and-pinion gear system was validated according to the ISO 6336:2019 standards to keep sufficient root safety and plank safety values which is depicted in Figure 1.

Results (basic calculation)			
Contact ratios	$[\varepsilon_{\alpha m}/\varepsilon_{\beta}/\varepsilon_{\gamma m}]$	1.751 / 0.000 / 1.751	
		Pinion	Rack
Actual tip circle (mm)	$[d_{ae}, H_z]$	32.000	50.000
Root safety		3.998	5.040
Flank safety		2.418	2.972
Safety against scuffing (integral temperature)		4.792	
Safety against scuffing (flash temperature)		99.516	

a)

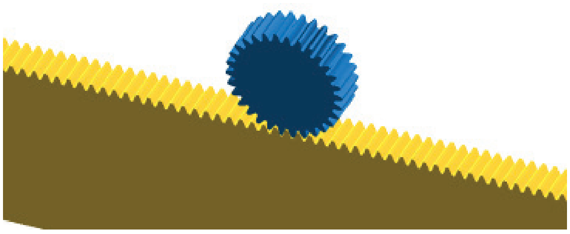

b)

Figure 1 - (a) Root safety and flank safety values for gear system, (b) Gear system simulation

The floater is connected to the internal rack in the PTO system. Therefore, the induced force on the rack is considered the same as wave induced force which is 332 N. The floater mass was selected as 30 kg to match the upward force and to ensure manageable handling for stable operation. Assuming a sinusoidal motion of the rack, the average absolute rack velocity was derived from the wave amplitude and wave period. The relationship between the pinion circular circumference (C), average linear velocity (v_{avg}), and the corresponding pinion speed (n_{avg}) is given as follows.

$$n_{avg} = \frac{60\, v_{avg}}{C} \qquad \ldots(3)$$

The average rotational speed of the pinion was approximately 64 RPM. The resulting torque on the pinion was estimated to be 4.7 Nm. Considering the average force induced on the rack system, an average mechanical power output nearing 31 W resulted. Therefore, the rated power output of the WEC was found to be 31 W under the defined wave conditions.

The counterweight helps the WEC to remain stationary and in contact with the seabed under both normal and extreme wave conditions. When considering extreme conditions, the counterweight (m_{cw}) must resist full buoyancy of the floater and ballast when compared to normal conditions. Therefore, the stability requirement can be expressed as follows.

$$\therefore m_{cw}g > (B_{ballast} + B_{floater}) - (m_{ballast}g + m_{floater}g) \ldots(4)$$

where "B" denotes buoyant force and "m" denotes mass. Major components of the WEC are depicted in Figure 2.

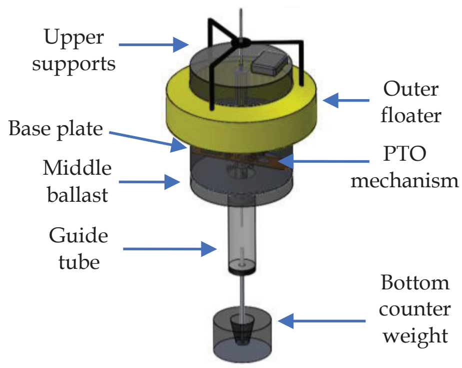

Figure 2 - WEC main components

4. Development of the WEC

4.1 Fabrication of PTO Mechanism

The PTO mechanism of the WEC is a dual rack and pinion system with motion rectifiers which contain one-way bearings to convert the bi-directional rotary movement of the generator shaft to a unidirectional movement. One-way bearings are fitted with each pinion to achieve this conversion. This enables the WEC model on capturing bidirectional motion of ocean waves. Here, module 1 rack and pinion gear were used which were previously validated according to the ISO 6336:2019 standards to ensure smooth performance.

4.2 Fabrication of Floater

The buoy-like floater was fabricated using high density Polyethylene (HDPE) to reduce weight. Metal sheets were wrapped in the inner circle to ensure a smooth surface while guide tubes were installed allowing vertical movement along the middle ballast. The floater was filled with PU expanding foam to maintain buoyancy even in the event of water ingress. Multiple outer sealing layers were added to ensure waterproofing and applied anti-corrosive coating to prevent corrosion.

4.3 Fabrication of Middle Ballast

The middle ballast was designed to house the PTO system, generator, battery, and associated electrical components. It was fabricated as a fully sealed steel structure, with an internal base plate welded to support both mechanical and electrical assemblies. External guide rails were added to align with the floater guides, ensuring smooth and strictly vertical motion during operation. The bottom guide tube was constructed from PVC and rigidly connected to the middle ballast. It includes an internal guide plate to support the PTO during operation. Outer sealing was performed to prevent water ingress and protect internal components.

4.4 Fabrication of Upper Supports

Upper supports provide a rigid connection between the outer floater and the internal rack gears of the PTO. The structure was fabricated using 1-inch box sections, with the floater and rack gears connected via steel plates and bolted joints, facilitating easy assembly, deployment, and maintenance. A four-bar configuration was employed to ensure uniform load distribution and enhanced structural stability.

4.5 Mechanical Losses

Several sources of mechanical losses are present in the WEC. Sliding and rolling contact between the rack and pinion teeth can result in frictional losses caused by tooth friction, minor misalignment, and inadequate lubrication. Additional losses arise from pillow block bearings and linear bearings, primarily due to shaft misalignment and friction within the rack guide system. The flexible coupling connecting the shaft to the generator may also contribute to mechanical losses as a result of elastic deformation and residual misalignment.

Furthermore, the outer floater moves along guide rails on the external surface of the ballast. Insufficient lubrication or uneven sliding at this interface can increase frictional resistance, leading to additional energy losses during WEC operation. Figure 3 depicts the fabrication process of certain components of the WEC.

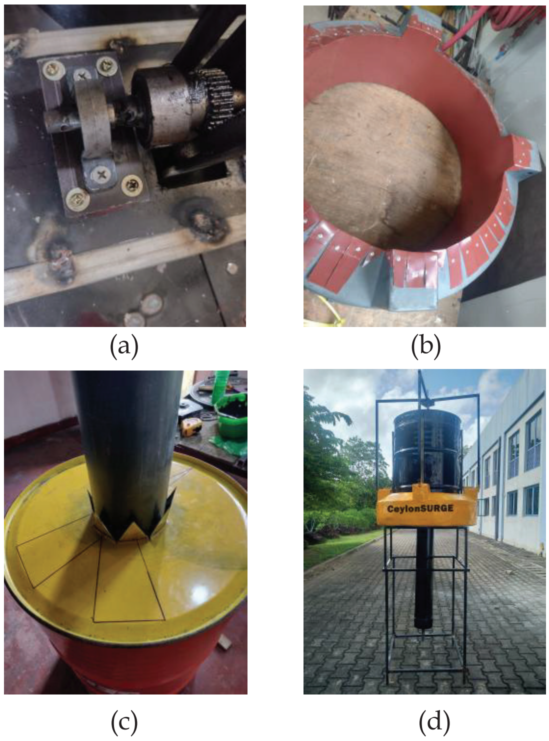

Figure 3 - (a) PTO fabrication, (b) Floater fabrication, (c) Middle ballast fabrication, (d) Final assembly

5. Electrical System

The electrical system of the WEC was designed to measure and monitor the current, voltage and power generated by the DC generator. The system includes sensors measuring voltage and current, with an ESP32-S3 microcontroller acting as the central data acquisition unit. The module collects sensor data and transmits to a cloud-based platform. Supporting components such as buck converters, capacitors, load resistors, and wiring ensure a stable and reliable operation. The basic electrical circuit of the WEC is represented in Figure 4.

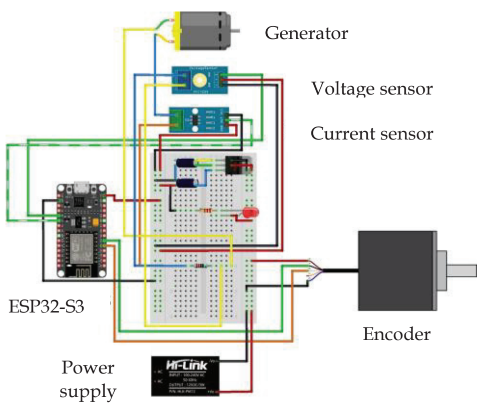

Figure 4 - Electrical circuit of the WEC

5.1 System Backend

The backend functions as an intermediary between the ESP32-S3 and Firebase. The backend receives real-time sensor data, validates the data, and calculates power output using the voltage-current relationship. After processing, the backend forwards verified data to the Firebase, ensuring a secure connection between hardware and cloud services.

5.2 Firebase

Firebase is used as a real-time cloud database which stores current, voltage and the calculated power values. As new data sets are received, the database updates instantly, enabling continuous, real-time data monitoring. This helps understand the performance of the WEC.

5.3 System Frontend

The frontend of the system is used to display real-time performance data of the WEC which is retrieved directly from the Firebase. The frontend contains numerical readings and graphical plots of current, voltage, and power, allowing users to conveniently observe the WEC performance and is depicted in Figure 5.

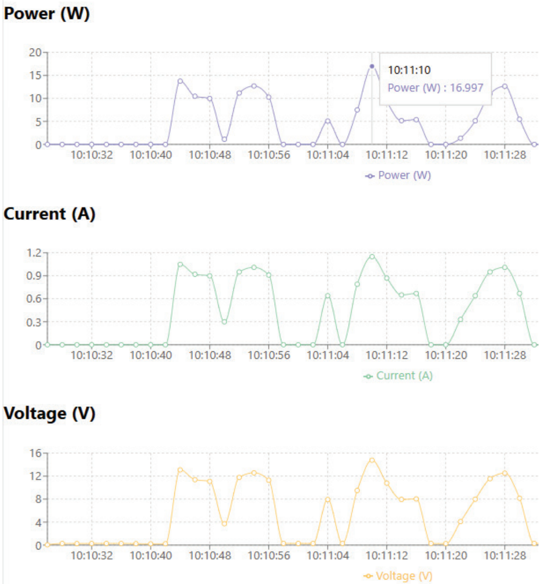

Figure 5 - Frontend - during manual testing

6. Hydrodynamic Simulations

Hydrodynamic simulations are considered as a key component of the validation process which enables evaluation of the floater response characteristics. Similar numerical investigations on heaving point absorber WECs have been reported using advanced hydrodynamic modelling approaches in order to analyse motion response and power capture performance [11]. These simulations guide optimal floater geometry selection. To evaluate the hydrodynamic performance and energy capture efficiency of the Ceylon SURGE Wave Energy Converter (WEC) floater, a Computational Fluid Dynamics (CFD) study was conducted using ANSYS AQWA (ANSYS 2025 R1 Student Version). As floater geometry significantly influences wave–structure interaction and power absorption, the analysis aimed to identify the most efficient floater shape for energy capture. Three geometries were investigated: cylindrical, hemispherical, and elliptical floaters, selected for both their distinct hydrodynamic behaviour and feasibility for fabrication and deployment.

To ensure a fair comparison, all simulations were performed under identical physical and boundary conditions. Each floater was designed with a constant inner diameter of 700 mm, outer diameter (or equivalent width) of 880 mm, and a total mass of 30 kg. Identical material properties, connection conditions, and wave excitation parameters were applied, with a uniform incident wave height of 0.2 m. The simulations evaluated the hydrodynamic response of each floater under the same wave conditions. Key output parameters included the Heave Response Amplitude Operator (RAO), phase variation, and initial hydrostatic force. These metrics were analysed to compare the relative hydrodynamic performance and energy capture potential of the three floater configurations. The simulation model of the cylindrical floater is displayed in Figure 6.

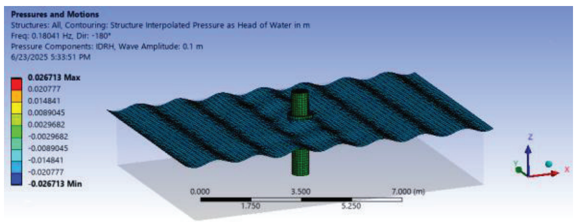

Figure 6 - Hydrodynamic simulation model of cylindrical floater in ANSYS AQWA

6.1 Heave Variation

In nearshore conditions, waves typically exhibit a broad frequency spectrum rather than a single dominant frequency. Consequently, a floater that demonstrates higher heave response over a wide frequency range is more suitable for effective energy extraction. Analysis graphs of the heave response results are shown in Figure 7, indicating that the cylindrical floater provides a consistently higher average heave motion compared to other configurations. This behaviour is primarily attributed to its larger water-plane area, resulting in stronger buoyancy variations and enhanced vertical motion under nearshore wave conditions.

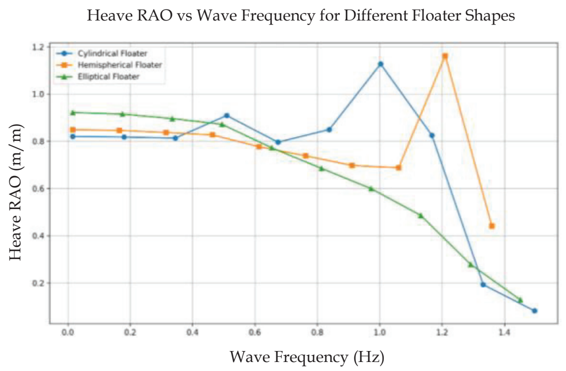

Figure 7 - Heave Response Amplitude Operator variation with wave frequency for cylindrical, hemi-spherical and elliptical floater shapes

6.2 Phase Variation

The phase variation describes the phase difference between wave excitation and the heave response of the floater, which is important for effective energy extraction. For efficient power capture, the heave velocity should be close to a 90° phase difference with respect to displacement as in the below Figure 8 [12]. The cylindrical floater maintains a phase angle closer to this optimal range over a wider frequency band compared to the hemispherical and elliptical floaters. This indicates better dynamic coupling with onshore waves and improved energy capture potential.

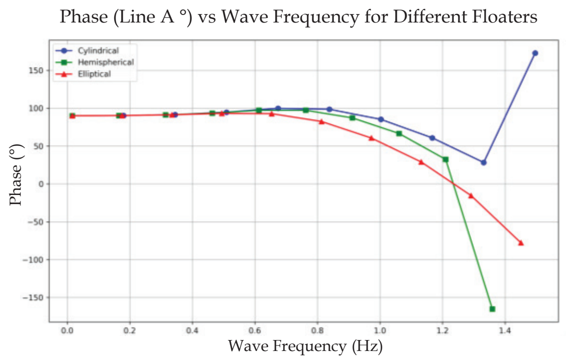

Figure 8 - Phase variation with wave frequency for cylindrical, hemi-spherical and elliptical floater shapes

6.3 Hydrostatic Force Variation

The hydrostatic force variation represents the initial buoyancy force acting on the floaters due to their submerged volume. The results show that the hemispherical floater experiences a higher initial hydrostatic force compared to the cylindrical and elliptical floaters, mainly due to its curved geometry and volume distribution. However, as the simulation progresses, the hydrostatic forces of all three floaters converge to similar steady values, indicating stable equilibrium conditions as in Figure 9.

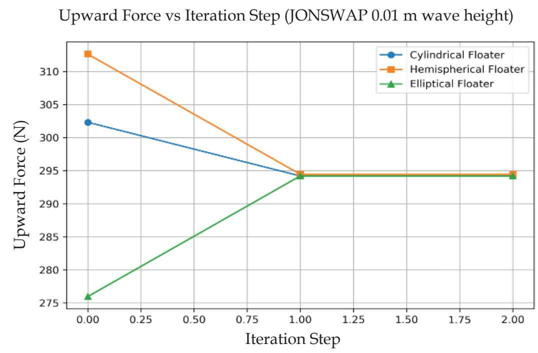

Figure 9 - Hydrostatic force variation with iteration step for cylindrical, hemi-spherical and elliptical floater shapes

The time-domain hydrostatic force variation obtained above for the cylindrical floater varies around 300 N which is reasonably close to the analytically calculated wave-induced force previously, confirming that selected area provides a realistic estimate of the forces acting of the WEC.

The buoy geometry was selected based on a comparative evaluation of key hydrodynamic performance indicators obtained from CFD simulations. Since the absorbed power of a point absorber is proportional to excitation force and heave velocity, geometries producing higher heave response amplitudes within the dominant frequency range are expected to yield greater energy capture. Accordingly, three criteria were used:

Average Heave RAO Magnitude: The mean RAO value was evaluated over the nearshore dominant frequency band (0.05–0.30 Hz). A higher RAO indicates stronger vertical displacement response to wave excitation, which directly increases heave velocity and the mechanical input available to the PTO system.

Phase Relationship: Phase difference between wave excitation and heave motion was analysed, as efficient energy extraction occurs when velocity is approximately 90° out of phase with excitation force. Geometries maintaining phase angles closer to this optimal condition across a broader frequency range were considered more favourable for energy absorption.

Hydrostatic Stability: Initial hydrostatic force and its convergence behaviour were examined to ensure stable equilibrium and predictable buoyancy characteristics. Stable hydrostatic response is essential for consistent oscillatory motion and reliable long-term operation.

Comparative analysis shows that the cylindrical buoy exhibited the highest average heave RAO across the considered frequency range, maintained phase angles closer to the optimal condition for power absorption, and demonstrated stable hydrostatic characteristics comparable to the other geometries. Although the hemispherical buoy exhibited a higher initial hydrostatic force, its reduced heave response and less favourable phase behaviour limited its energy capture effectiveness. The elliptical geometry similarly showed lower average RAO values. Since absorbed power in point absorber systems scales approximately with heave velocity, which is proportional to displacement amplitude, the cylindrical geometry was determined to provide the most favourable hydrodynamic performance for nearshore wave energy extraction, therefore selecting it as the optimal buoy configuration for the WEC.

6.4 Time Domain Analysis

In the time-domain analysis, an irregular wave was defined using the JONSWAP spectrum to simulate realistic sea conditions. The irregular wave condition was defined using the JONSWAP (Joint North Sea Wave Project) spectral formulation [13], expressed as:

$$S(\omega) = \frac{\propto g^2}{\omega^5} exp\left(-\frac{5}{4}\left(\frac{\omega_P}{\omega}\right)^4\right)\gamma^{exp\left(-\frac{(\omega-\omega_\rho)^2}{2\sigma^2\omega_p^2}\right)} \quad \ldots. (5)$$

where,

$S(\omega)$ = spectral density (m² ·s),

α = Phillips's constant (spectral scaling parameter),

g = gravitational acceleration (9.81 m/s²),

ω = angular frequency (rad/s),

ω_p = peak angular frequency (rad/s),

γ = peakedness factor, and

σ = spectral width parameter (0.07 for $\omega \leq \omega_p$, and 0.09 for $\omega > \omega_p$).

The wave period range was set from 5 s to 25 s, with a significant wave height of 0.2 m, representing calm sea states. A gamma value (a peakedness factor γ=2 was selected to represent moderate sea states, typical of nearshore conditions) [14] was used to sharpen the spectrum, and a peak period of 16 s concentrated energy in long-period swells, capturing realistic irregular wave behaviour. Wave surface elevation was generated over 300 seconds based on these conditions. Here, peak period T_p=16s (corresponding to a frequency of 0.0625 Hz) was adopted to evaluate the WEC response under long-period swell conditions. Although nearshore wave measurements along southern coast of Sri Lanka commonly show dominant wave periods in the range of approximately 6–12 s [15], longer-period swells exceeding 14 s can occur, particularly during monsoonal transitions and distant storm events. Therefore, the selected peak period represents a conservative swell-dominated scenario intended to assess the hydrodynamic behaviour of the device beyond the primary wind-wave frequency band. Future studies will incorporate site-specific measured wave spectra for enhanced regional accuracy. The wave surface elevation to time graph is depicted in Figure 10.

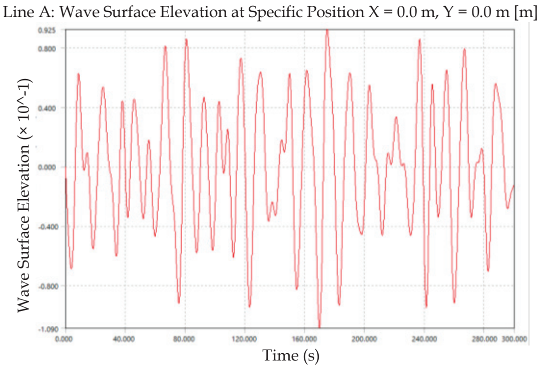

Figure 10 - Wave surface elevation time history generated using the JONSWAP spectrum under irregular wave conditions

Heave RAO variations of cylindrical, hemispherical, and elliptical floater shapes were analysed under the above irregular wave conditions. The heave RAO responses of the floater shapes show clear differences under the same irregular wave condition. The cylindrical floater exhibits the largest heave motions with sharp peaks as per in Figure 11.

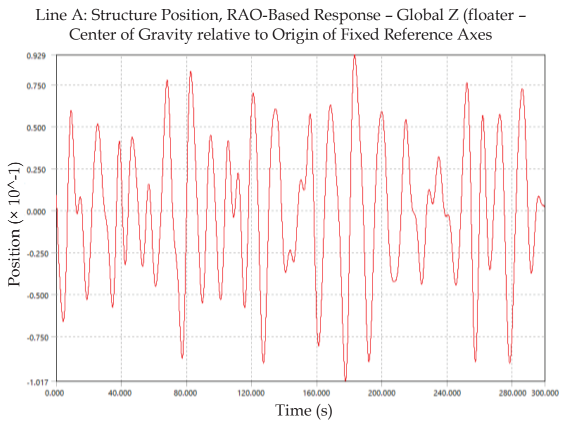

Figure 11 - Time-domain heave response of the cylindrical floater under irregular wave excitation

7. Deployment of the WEC

The WEC was deployed for real-world sea trials at the Old Harbour premises in Galle, Sri Lanka (6.029230° N, 80.219010° E). On the trial date, the prevailing wave conditions were characterized by wave heights of 0.1–0.5 m and a dominant wave frequency of approximately 0.1 Hz. This location was selected due to its consistent nearshore wave conditions, operational safety, accessibility for deployment and monitoring, and availability of logistical resources. The site had a water depth of 2.2 m, which closely matched the WEC's optimal operating height, supporting stable performance during testing.

The deployment of the Ceylon SURGE WEC involved transporting the middle ballast and counterweight to the shoreline, assembling them on a modular pontoon, and securing the system with ropes to ensure stability during transport. At the deployment location, the counterweight was first submerged to stabilize the structure, followed by the installation of the outer floater. This sequence enabled on-site assembly under controlled conditions while minimizing structural loads during deployment. The deployment procedure is shown in Figure 12.

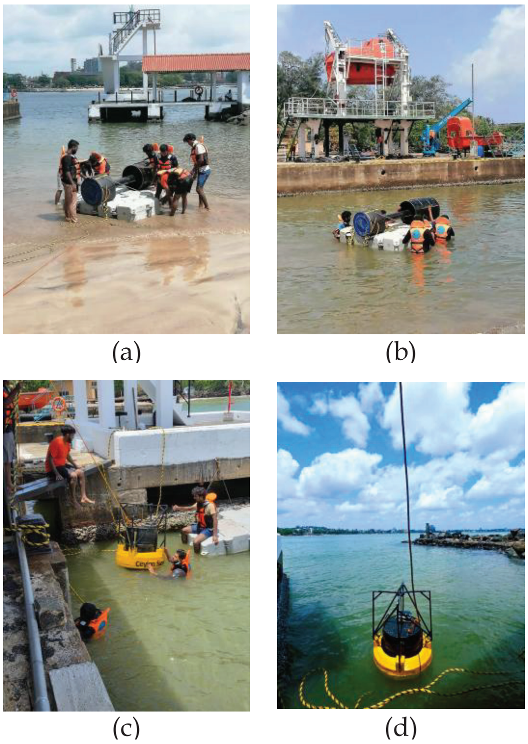

Figure 12 - (a) Assembling device on floating pontoon, (b) Transporting to deployment location, (c) Floater insertion, (d) Successfully deployed Ceylon SURGE WEC

8. Field Test Results

The WEC was deployed in the old harbour premises, Galle and data was collected for the current, voltage and power for nearly 3.5 hours. The following Figure 13 indicates the resulting graphs of the data collection.

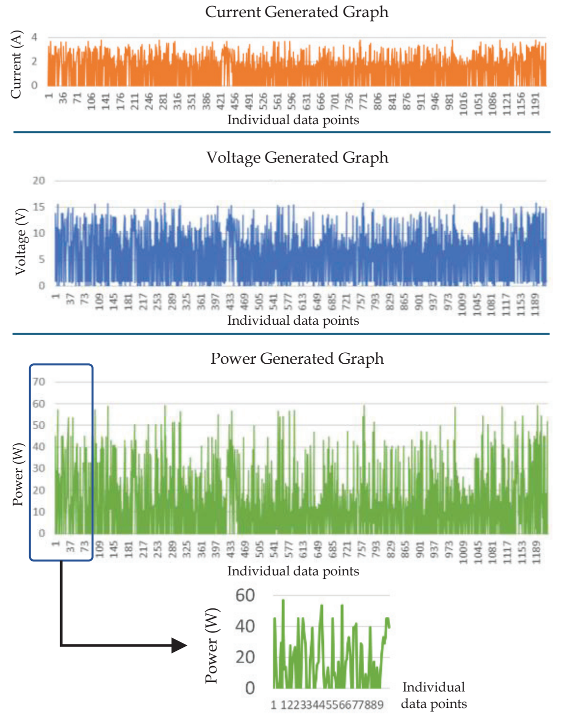

Figure 13 - Experimental results collected from sea trial

The spike-like behaviour observed in the power generation profile is attributed to the irregular and instantaneous nature of ocean waves. Variations in wave amplitude and particle velocity result in transient increases in available wave power, causing short-duration peaks in the generated power. Under high-amplitude and high-velocity wave conditions, the WEC reaches its maximum power output. From the recorded power data, the Ceylon SURGE WEC achieved a maximum power output of 59.22 W. Due to the intermittent nature of power generation, the average power output was also evaluated, yielding a value of 15.03 W. The incorporation of capacitors or energy storage elements could mitigate power fluctuations by temporarily storing excess energy during peak generation periods and releasing it during low-output intervals.

The overall efficiency of the WEC was estimated by comparing the average extracted power with the available wave power per crest [16]. Based on the measured average power output, deployment location, and prevailing wave conditions, the conversion efficiency of the Ceylon SURGE WEC was calculated to be approximately 8.51%. Real-world testing of the WEC is depicted in Figure 14.

Figure 14 - Operating of Ceylon SURGE WEC

The measured average mechanical power of approximately 15 W is lower than the analytically predicted value. This reduction is expected and can be caused due to various reasons such as mechanical losses in PTO mechanism, friction losses in guide mechanism, hydrodynamic damping not fully being captured in analysis, generator inefficiencies and other aspects. Also, irregular sea states and non-ideal wave conditions during real-world sea trials may contribute to the reduction of energy captured compared to the theoretical monochromatic wave assumption. Despite the losses, the experimental results confirm that the WEC model operates as intended and produces power within the same order of magnitude as the analysed values, thereby validating the overall WEC design methodology and the analytical framework.

9. Conclusion

This study successfully developed and validated a double-buoy, point absorber type WEC, Ceylon SURGE, optimized for southern Sri Lankan wave conditions, following an analytical, numerical and experimental framework. Hydrodynamic simulations conducted using ANSYS AQWA identified the cylindrical floater as the optimal geometry. Subsequent field testing of the WEC confirmed a stable operation, achieving a peak power output of 60 W and an average power output of 15 W, validating both mechanical and electrical designs. These results highlight the device's suitability for low-to-moderate wave climates.

A key feature of the Ceylon SURGE is its fully sealed subsurface architecture, which protects critical internal components from seawater exposure, reducing the risk of water ingress which is a common failure mode in WECs. This design enhances long-term reliability and minimizes maintenance, providing a distinct advantage over existing WEC concepts.

Although the current study focused on a prototype, the observed performance establishes a strong foundation for future development. The WEC design supports scalability, enabling optimization through dimensional scaling and refinement of the dual rack-and-pinion PTO mechanism. With further development, full-scale Ceylon SURGE WECs could provide a reliable renewable energy source for coastal communities and represent a promising approach to advancing nearshore wave energy utilization in maritime regions.

10. Future Work

Future research on Ceylon SURGE will focus on advancing the WEC to full-scale deployment. Device scaling will be carried out using Froude similarity laws to maintain dynamic similarity between the model and the prototype. Scaling up [17] will require modifications to key parameters, including buoy dimensions, mass, PTO capacity, gear system, and structural strength, enabling higher power outputs suitable for grid connection and stability. At full scale, significantly higher power output is expected. Deployment of multiple scaled-up WECs in arrays or wave farms can further increase total energy production, allowing shared infrastructure and maintenance, thereby reducing overall costs. In addition, integrating WECs with offshore wind farms offers the potential for hybrid renewable energy systems, improving power supply consistency. Future work will also investigate eliminating the bottom counterweight and introducing a reaction plate, enabling deployment across a wider range of sea depths. The reaction plate will replace the stabilizing function of the counterweight while maintaining stability.

Large-scale deployment of Ceylon SURGE along the Sri Lankan coast could support energy diversification, coastal economic development, and reduced dependence on fossil fuels. Further research will focus on reducing the levelized cost of energy (LCOE) [18] through design simplification, enhanced PTO efficiency, improved reliability, and the use of locally available and sustainable materials. As LCOE depends on multiple factors such as device type, deployment location, and system configuration [19], addressing these aspects considering the lifecycle and environmental impact of the WEC will be essential for long-term sustainability.

References

1. Ocean Energy Europe. "Wave energy." [Online]. Available: https://www.oceanenergy-europe.eu/ocean-energy/wave-energy/ . [Accessed: 21-Dec-2025].
2. Zatkos, L. "The Promise and Pitfalls of Wave Power." [Online]. Available: https://www.earthisland.org/journal/index.php/articles/entry/promise-pitfalls-wave-power-renewable-energy/
3. Esteban, D. J.-S. L.-G., and Morales, V. N. "Classification of Wave Energy Converters." Juniper Publishers, 2017.
4. G_Bioenergy, "Pros And Cons Of Renewable Wave Energy: Some Bullet Points." [Online]. Available: https://www.globalbioenergy.org/renewable-wave-energy-pros-and-cons/
5. Karunarathna, H., Maduwantha, P., Ratnasooriya, H., De Silva, K., and Kamranzad, B. "Wave Power Potential of Sri Lanka." Engineer: Journal of the Institution of Engineers, Sri Lanka, Vol. 54, No. 2, p. 1, Aug. 2021. doi:10.4038/engineer.v54i2.7404
6. Li, T. A., and Li, H. "Ocean Wave Energy Converters: Status and Challenges." MDPI, 2018.
7. Seneviratne, I. H. D., et al. "Design, Development, and Field Testing of a Scalable Nearshore Wave Energy Converter Optimized for Sri Lanka's Shallow Sea Conditions." Engineer: Journal of the Institution of Engineers, Sri Lanka, Vol. 59, No. 1, pp. 123–132, Feb. 2026. doi:10.4038/ENGINEER.V59I1.7738
8. Jayathunga, B. J. C. L., and Karunasena, H. C. P. "Development and Performance Analysis of a Small-Scale On-shore Wave Energy Converter." Engineer: Journal of the Institution of Engineers, Sri Lanka, Vol. 55, No. 4, p. 47, Dec. 2022. doi:10.4038/ENGINEER.V55I4.7543
9. Mendez, F. J., and Losada, I. J. "An Empirical Model to Estimate the Propagation of Random Breaking and Nonbreaking Waves Over Vegetation Fields." Coastal Engineering, Vol. 51, No. 2, pp. 103–118, Apr. 2004. doi:10.1016/j.coastaleng.2003.11.003
10. Falnes, J. Ocean Waves and Oscillating Systems: Linear Interactions Including Wave-Energy Extraction. Cambridge University Press, UK, 2020.
11. Manawadu, N. H. D. S., Nissanka, I. D., and Karunasena, H. C. P. "SPH-Based Numerical Modelling and Performance Analysis of a Heaving Point Absorber Type Wave Energy Converter with a Novel Buoy Geometry." Renewable Energy, Vol. 228, p. 120595, Jul. 2024. doi:10.1016/j.renene.2024.120595
12. Berrio, Y., et al. "Development and Hydrodynamic Performance of an Oscillating Buoy-Type Wave Energy Converter." Energies, Vol. 18, No. 16, p. 4383, Aug. 2025. doi:10.3390/en18164383
13. WikiWaves. "Ocean-Wave Spectra." [Online]. Available: https://www.wikiwaves.org/index.php/Ocean-Wave_Spectra
14. Falcão, A. F. de O. "Wave Energy Utilization: A Review of the Technologies." Renewable and Sustainable Energy Reviews, Vol. 14, No. 3, pp. 899–918, Apr. 2010. doi:10.1016/j.rser.2009.11.003
15. Karunarathna, H., et al. "Evaluation of Spatio-Temporal Variability of Ocean Wave Power Resource Around Sri Lanka."
16. Falnes, J., and Kurniawan, A. Ocean Waves and Oscillating Systems: Linear Interactions Including Wave-Energy Extraction, 2nd ed. Cambridge University Press, 2020. doi:10.1017/9781108674812
17. Jin, S., Zheng, S., and Greaves, D. "On the Scalability of Wave Energy Converters." Ocean Engineering, Vol. 243, Jan. 2022. doi:10.1016/j.oceaneng.2021.110212
18. Chen, B., Luan, Z., He, G., He, R., and Liu, C. "Techno-Economic Assessment of Wave Energy Converters Arranged on an Octagonal Platform using Multiple Financial Parameters." Renewable Energy, Vol. 256, p. 123906, Jan. 2026. doi:10.1016/j.renene.2025.123906
19. Seneviratne, H., Karunasena, C., and Amlashi, H. "A Multi-Dimensional Review on Performance Enhancement Opportunities of Next Generation Wave Energy Converters." Proceedings of the European Wave and Tidal Energy Conference, Vol. 16, Sep. 2025. doi:10.36688/ewtec-2025-850